

1 Plasma reforming of tar model compound in a rotating gliding arc reactor: 2 Understanding the effects of CO₂ and H₂O addition

3 Fengsen Zhu^{a, b, c, 1}, Hao Zhang^{a, 1, *}, Haiping Yang^d, Jianhua Yan^a, Xiaodong Li^{a, *}, Xin Tu^{b, *}

4 ^a State Key Laboratory of Clean Energy Utilization, Zhejiang University, Hangzhou 310027, China

5 ^b Department of Electrical Engineering and Electronics, University of Liverpool, Liverpool L69 3GJ,
6 UK

7 ^c Zhejiang Electric Power Design Institute Co. Ltd, Hangzhou 310012, China

8 ^d State Key Laboratory of Coal Combustion, School of Energy and Power Engineering, Huazhong
9 University of Science and Technology, Wuhan 430074, China

10
11 **Abstract:** In this study, a rotating gliding arc (RGA) plasma reactor co-driven by a magnetic field
12 and tangential flow has been investigated for the reforming of toluene as a tar surrogate from the
13 gasification of biomass or waste. The effect of steam and CO₂ addition on the reaction performance
14 of the plasma tar reforming process has been evaluated in terms of the conversion of toluene, gas
15 production and energy efficiency. The presence of CO₂ in the reaction suppresses the conversion of
16 toluene. By contrast, adding an appropriate amount of steam to the reforming process significantly
17 enhances the conversion of toluene, while further increasing steam concentration reduces the
18 conversion of toluene. The maximum toluene conversion of 85.2% is achieved at an optimal steam
19 concentration of 16%. Optical emission spectroscopic (OES) diagnostics have been used to
20 understand the generation of reactive species contributed to the conversion of toluene and reaction
21 intermediates in the plasma reforming process. The possible reaction pathways and mechanisms have

¹ The first two authors contributed equally to this work.

* Corresponding authors.

E-mail addresses: zhang_hao@zju.edu.cn (H. Zhang), lixd@zju.edu.cn (X. D. Li), xin.tu@liv.ac.uk (X. Tu)

1 been discussed based on the analysis of gases and condensed liquid by-products combined with the
2 emission spectra of the plasma in the presence or absence of steam and CO₂.

3 **Keywords:** Tar reforming; toluene; rotating gliding arc; non-thermal plasma; mechanisms

4

5

6 **1. Introduction**

7 The increasing depletion of fossil fuels and growing awareness of global warming is pushing up
8 the development of biomass or municipal solid waste (MSW) utilization technology [1, 2].
9 Gasification, which is performed by partial oxidation of the carbon contained in biomass or MSW
10 with a controlled oxidant amount, is considered as one of the most sustainable and promising
11 thermochemical processes for biomass and MSW utilization. Gasification enables a high-efficiency
12 conversion of biomass or MSW into value-added syngas mainly consisting of H₂, CO and CH₄,
13 providing high flexibility for the generation of heat and electricity, or the synthesis of value-added
14 platform chemicals and synthetic fuels [3, 4]. However, the producer gas is inevitably contaminated
15 by some undesired impurities, such as tars, particulates, alkali metals and acid gases, of which the
16 contamination by tars is a key challenge in the gasification of biomass or waste. As the presence of
17 tars in the producer gas can cause fouling, obstruction and corrosion in downstream equipment,
18 limiting the use of producer gas for energy applications [5-7].

19 Tar is a generic complex mixture of condensable hydrocarbons, including aromatics as well as
20 multiple ring polycyclic aromatic compounds (PAHs) that may contain hetero-atoms, such as sulphur
21 and nitrogen, and may be partly oxidized. A widely accepted definition of tar refers to ‘all organic
22 contaminants with a molecular weight larger than benzene’ [8]. Typically, the tar content of producer
23 gas varies from 0.5 to 100 g/Nm³, depending on the type of gasifiers, with a co-current flow of fuel

1 and oxidant minimizing tars and counter-current operation favouring fuel economy, yet producing
2 dirtier gas, since it contains the volatile matter of the feedstock. Most applications of producer gas
3 require a low tar content. For instance, the tolerance of internal combustion engines for tars is well
4 below 100 mg/Nm³. As for gas turbines, this constraint becomes even stricter, with a limit of 5
5 mg/Nm³ [8-10]. Thus, effective removal and conversion of tars from raw producer gas are of great
6 importance for the gasification process.

7 Removing tars from producer gas can be accomplished through mechanical separation, including
8 filters, cyclones, scrubbers, and electrostatic precipitators [10]. Physical methods may remove part of
9 tars together with captured particulates. However, the chemical energy contained in the tars is lost,
10 reducing the efficiency of the gasification process. Additionally, wet gas cleaning generates large
11 amounts of contaminated water, requiring downstream treatment or recycling [5, 11]. Thermal or
12 catalytic cracking can convert tars into light gases. However, high temperatures (>1000 °C) are
13 required for thermal cracking to achieve sufficient tar destruction in a realistic residence time [12],
14 incurring high energy cost and production of agglomerated soot particles [13]. Catalytic cracking can
15 operate at the temperature of the gasifier [10]. Various catalysts have been explored for tar reforming,
16 including Ni- or other metal-based catalysts, basic and acid catalysts, and activated carbon [14-19].
17 Unfortunately, most catalysts can be easily fouled by coke formation or poisoned by sulphur and
18 chlorine compounds. Finding cost-effective and stable catalysts remains a major challenge for
19 catalytic cracking of tars from gasification.

20 Non-thermal plasmas have been regarded as a promising technology for the effective destruction
21 and conversion of tars from the gasification of biomass or MSW. Plasmas are normally subdivided
22 into thermal plasma and non-thermal plasma. Thermal plasma has a gas temperature of higher than
23 10⁴ K but lacks chemical selectivity because of the equilibration state between the electrons and heavy

1 gas molecules. In non-thermal plasmas, the gas temperature (normally lower than 1500K) is much
2 lower in comparison to the electron temperature (normally 1-5 eV, $1\text{eV} \approx 10^4\text{ K}$), which means the
3 energy input can be used to promote specific chemical reactions without heating the system. In a non-
4 thermal plasma process, reactive species such as energetic electrons, ions, free radicals, excited
5 molecules or atoms, are present and initiate a variety of chemical reactions [20-23]. In addition, the
6 plasma reforming process can be switched on and off quickly due to its instant reaction initiation with
7 a high reaction rate. Moreover, non-thermal plasma can operate under mild conditions (atmospheric
8 pressure and low temperature) and shows the merits of low investment and easy operation etc.
9 However, very limited efforts have been devoted to the investigation of tar reforming using non-
10 thermal plasmas. A few non-thermal plasma processes have been proposed for the conversion of
11 model tar compounds (e.g., toluene and naphthalene) using nitrogen as a carrier gas, including corona
12 discharge [24, 25], microwave discharge [26], dielectric barrier discharge (DBD) [27] and gliding arc
13 (GA) discharge [28, 29]. These studies demonstrated the promising potential of using non-thermal
14 plasma processes for tar reforming, but still facing challenges such as carbon deposition,
15 polymerization, low processing capacity and low energy efficiency. Moreover, the influence of
16 oxidative components (e.g. steam and carbon dioxide), which exist intrinsically in the producer gas,
17 on the plasma reforming of tar model compounds is still unclear. Significant fundamental researches
18 are still required to further enhance the conversion of tars and energy efficiency of the process through
19 the design and development of new reactor concepts with enhanced processing capacity and flexibility.

20 Among different non-thermal plasma systems, gliding arc discharge is one of the most attractive
21 because it can simultaneously provide a relatively high energy density, high electron temperature,
22 good chemical selectivity, and low energy consumption [30-32], providing high flexibility to work in
23 a wide range of reactant flow rates (up to 20 L/min in laboratory scale) and plasma power levels (up

1 to several kW) [33]. However, in a traditional flat gliding arc discharge that consists of two divergent
2 knife-shaped electrodes, the feed flow rates have to be quite high (e.g., 10-20 L/min) to maintain the
3 gliding arc, which thus leads to a short residence time of reactant [34-36]. More importantly, a quasi-
4 two-dimensional plasma reaction area that is confined by the flat electrodes leads to a limited fraction
5 of the gas flow that processed by the plasma (e.g., around 20% depending on the reactor geometry)
6 [36, 37].

7 To solve these problems, three-dimensional rotating gliding arc (RGA) reactors have been
8 proposed, which can be driven by either magnetic field [38] or tangential flow [39]. Compared with
9 traditional flat gliding arc discharge, the RGA reactor could provide a stable and large three-
10 dimensional plasma zone for chemical reactions by creating a rotating “plasma disc” area with certain
11 axial thickness. In this way, the plasma area can be enhanced with an elongated residence time of
12 reactants. In this study, an updated rotating gliding arc plasma reactor co-driven by a magnetic field
13 and tangential flow has been developed for the conversion of toluene as a tar surrogate from
14 gasification. Toluene is commonly studied as a model tar compound both in plasma process [27, 28,
15 40, 41] and in traditional reforming process [42, 43], as it is stable and a good representative of
16 aromatic compound. In addition, it is less harmful and has a simple structure and low boiling point,
17 thus offering convenience for a good performance of the experiments. The RGA reactor can generate
18 a synergetic effect resulted from the combination of a swirling flow and a Lorentz force, providing a
19 steadier rotating arc volume with enhanced rotation frequency (up to 100 rotations per second) over
20 a wider flow rate range (e.g., 0.05-40 L/min) [44]. It has been evidenced that the arc stability and
21 rotating frequency can be increased under the effect of Lorentz force or swirling flow [45, 46]. Our
22 previous study showed that the RGA reactor could provide a maximum tar conversion of over 95%,
23 in a toluene destruction process in N₂ flow [47]. H₂ and C₂H₂ are the major gas products with

1 selectivity of up to 39.4% and 27.0%, respectively.

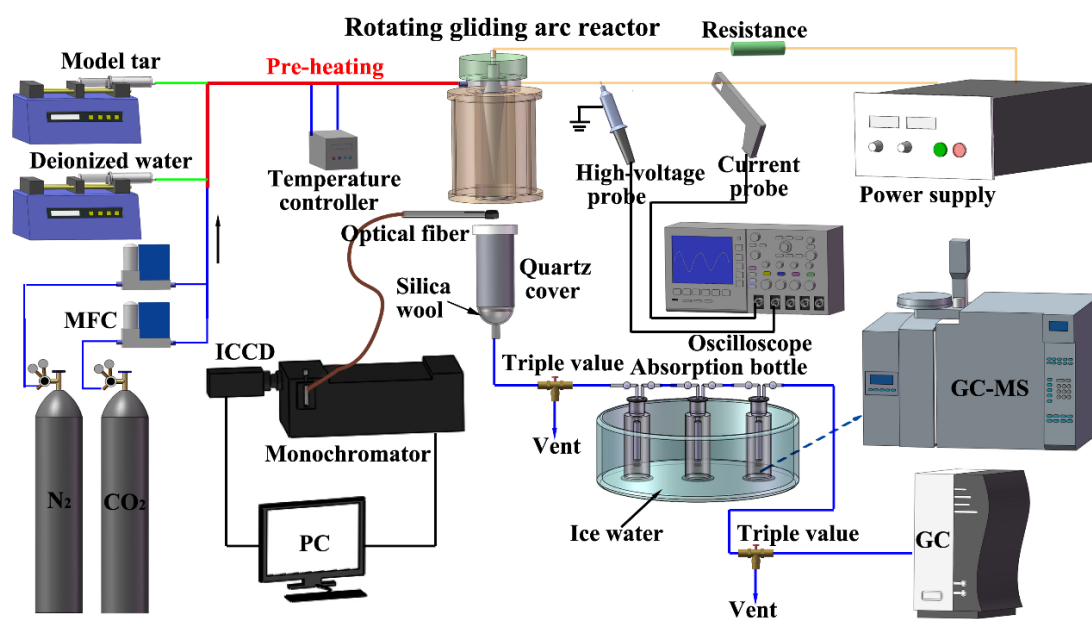
2 It is well known that steam and carbon dioxide exist intrinsically in the producer gas with high
3 content, and thus can react with tar compounds. However, the effects of steam and carbon dioxide on
4 the reaction performance of plasma tar destruction have been scarcely investigated. Therefore, this
5 work aims to evaluate the performance of the attractive RGA plasma system for model tar compound
6 reforming in the oxidative atmosphere, with a specific focus on the effect of steam and carbon dioxide.
7 Optical emission spectroscopic (OES) diagnostics have been used to get new insights into the
8 formation of a range of reactive species generated in the plasma reforming process in the presence
9 and absence of steam and CO₂. The plausible reaction pathways and mechanisms in the plasma
10 reforming of tar model compound have been proposed and discussed based on the analysis of gas and
11 liquid products combined with OES diagnostics. These works are expected to advance the industrial-
12 scale application of this promising process.

13

14 **2. Experimental**

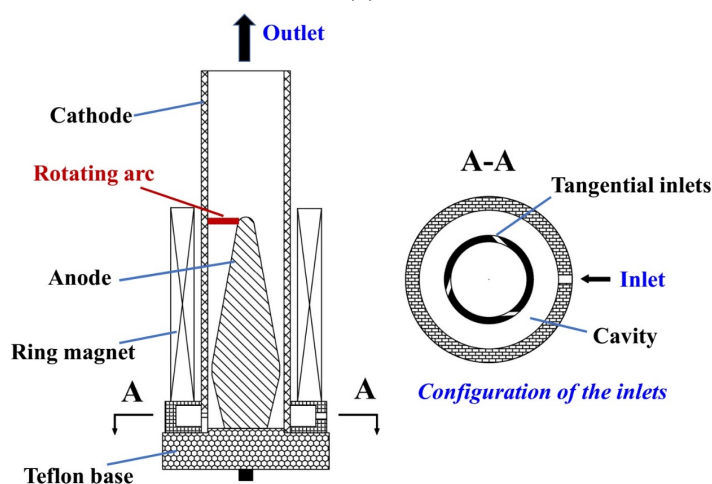
15 **Equipment.** Fig. 1 shows the schematic diagram of the experimental set-up. The RGA reactor
16 comprises a plasma reaction zone generated between a conical inner electrode (anode) and a
17 cylindrical grounded outer electrode (cathode), while both electrodes are fixed coaxially and insulated
18 by a Teflon base. A ring magnet is placed outside the cylindrical cathode, generating an upward
19 magnetic field to stabilize and accelerate the arc. The gas mixture is injected into the RGA reactor
20 through three tangential inlets and swirls as a cyclonic flow around the inner electrode. The arc is
21 ignited initially at the narrowest gap (2 mm) between the electrodes and then starts rotating rapidly
22 under the combined effect of a swirling flow and a Lorentz force, generating a stable three-
23 dimensional plasma arc zone for chemical reactions. A more detailed description of the RGA reactor

1 can be found in our previous works [47].



2
3

(a)



(b)

Fig. 1. Schematic diagram of the RGA plasma experimental setup (a) and the RGA reactor (b).

7

8 **Feed.** As shown in Fig. 1, the flow of toluene (purity $\geq 99.5\%$, J.T. Baker) solvent and deionized
9 water is controlled by high-resolution syringe pumps (Harvard, 11 plus) and injected into a preheated
10 ($200\text{ }^{\circ}\text{C}$) stainless-steel pipe, generating a steady-state vapour flow mixed with a nitrogen flow before
11 injected into the RGA reactor.

12 **Power supply – Optical measurement.** The RGA reactor is connected to a DC power supply

1 (Teslaman TLP2040) with a maximum peak voltage of 10 kV. A resistance of 40 k Ω is connected to
2 the power supply in series to limit the current. The arc voltage and current waveforms are recorded
3 by a digital oscilloscope (Tektronix DPO4034B). An optical fibre is placed at 6 cm above the plasma
4 arc to record the emission spectra of the RGA by using an emission spectrometer equipped a 750-mm
5 monochromator (PI-Acton 2750) and an intensified charge-coupled device (ICCD) (PI-MAX 2,
6 512 \times 512 pixel). Note the plasma arc is rotating rapidly and is dynamic. Thus, the collected spectra
7 represent the integrated intensity of the plasma emission along the line-of-sight across the “plasma
8 disc”, as similarly reported in other works [48-50].

9 **Analysis of liquid and gaseous products.** In the plasma reforming of tar, three successive
10 absorption bottles are placed in an ice water bath to condense and collect unconverted toluene and
11 condensable by-products generated in the reaction. The first two bottles contain hexane solvent to
12 absorb condensable products and the last one is kept empty to collect entrained droplets. The collected
13 liquid samples are qualitatively analyzed using a gas chromatography-mass spectrometry (GC-MS,
14 Agilent 6890N GC/5975B MSD), while the gaseous products are quantitatively measured by a gas
15 chromatograph (GC, Agilent 490 Micro GC; columns: MS5A 10m BF and PPU 10m BF; carrier gas:
16 helium and argon). 5 Standard solutions of toluene/hexane (500 to 3000 mg/L) were used for
17 obtaining the calibration curves of toluene. In each experiment, the collected liquid sample in a
18 specific experimental period was diluted with hexane to 100 ml, to quantify the unconverted toluene
19 in the product.

20 **Test program.** To evaluate the effect of CO₂, steam and their combination on the plasma reforming
21 of toluene, four experiments are carried out using different gas compositions: I. N₂ + CO₂ (0-36%),
22 II. N₂ + 16% H₂O + CO₂ (0-36%), III. N₂ + H₂O (0-24%) and IV. N₂ + 12% CO₂ + H₂O (0-24%). The
23 total flow rate is fixed at 0.6 Nm³/h with an input toluene concentration of 10 g/Nm³, unless otherwise

1 specified. As the inert carrier gas N₂ can be considered as unreacted in the process, the outlet gas flow
 2 rate is calculated based on the inlet N₂ flow rate and the detected N₂ concentration in the effluent gas.
 3 The discharge powers under the studied conditions were 375 ± 20W for Test I, 410 ± 5W for Test II,
 4 400 ± 25W for Test III, 410 ± 40W for Test IV.

5 The conversion of toluene and energy efficiency of the plasma process are defined as:

$$6 \quad \text{Conversion (\%)} = \frac{[C_7H_8]_{in} - [C_7H_8]_{out}}{[C_7H_8]_{in}} \times 100\% \quad (1)$$

$$7 \quad \text{Energy efficiency (g/kWh)} = \frac{\text{grams of toluene converted per min}}{P(W) \times 60/3600000} \quad (2)$$

8 where [C₇H₈] is the moles of toluene (mol) and P is the discharge power (W).

9 Note that the power consumed on the temperature controller was not taken into account in the
 10 calculation of energy efficiency, in consistence with similar works [13, 27, 51].

11 The carbon balance is determined by:

$$12 \quad \text{Carbon balance (\%)} = \frac{7[C_7H_8]_{out} + [CO_2]_{out} + [CO]_{out} + \text{sum of } x[C_xH_y]_{out}}{7[C_7H_8]_{in} + [CO_2]_{in}} \times 100\% \quad (3)$$

13 where [CO₂]_{out} and [CO]_{out} are the moles of CO₂ and CO in the effluent gas; [C_xH_y] indicates the
 14 moles of CH₄, C₂H₂, C₂H₄ or C₂H₆ in the effluent gas. Note that the generated liquid by-products
 15 (trace amounts) and the solid carbon, which cannot be quantified in this work, are not taken into
 16 account in the carbon balance calculation.

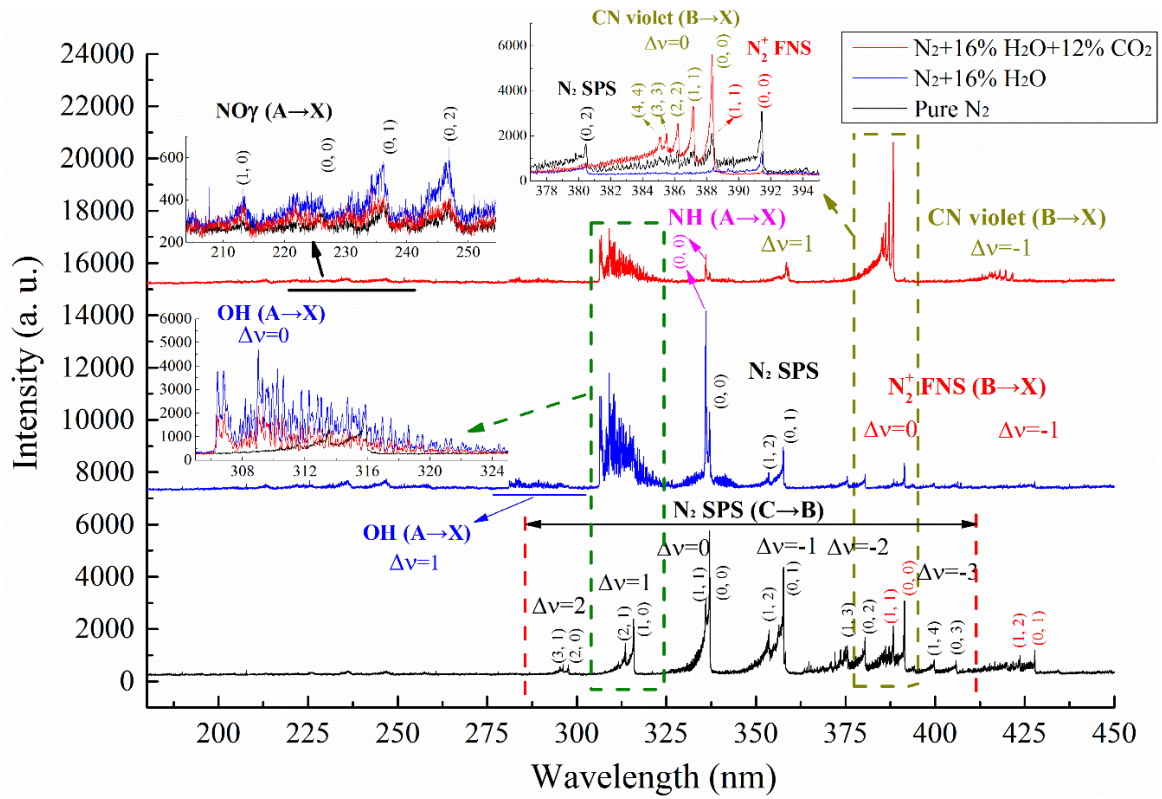
17

18 **3. Results and discussion**

19 **3.1 OES diagnostics of the RGA plasma**

20 Optical emission spectroscopy diagnostics have been used to understand the formation of reactive
 21 species generated by the RGA plasma using different carrier gas compositions and to get new insights
 22 into the possible reaction mechanisms and pathways in the plasma reforming of toluene. Typical

1 emission spectra of the RGA plasma with different carrier gas compositions are shown in Fig. 2.



2
3 Fig. 2. The OES spectra observed for different carrier gas composition.

4
5 **Nitrogen.** The spectrum of the N₂ RGA is dominated by the second positive system (SPS) of N₂
6 bands $C^3\Pi_u(v'') \rightarrow B^3\Pi_g(v'')$ and the first negative system (FNS) of N⁺ bands $B^2\Sigma_u^+(v') \rightarrow X^2\Sigma_g^+(v'')$.
7 Besides, several weak ($A^2\Sigma^+(v') \rightarrow X^2\Pi(v'')$) bands of NO_γ also appear at 210–250 nm, possibly
8 because of the presence of a trace impurity in the gas. The detected bands confirm the presence of
9 nitrogen molecules N₂^{*} at different excited states (N₂(A³Σ_u⁺), N₂(B³Π_g) and N₂(a¹Σ_u⁻), etc.); these
10 are vital for initiating and driving reactions.

11 **N₂/H₂O plasma.** In the N₂/H₂O plasma, in addition to the N₂ SPS bands, N₂⁺ FNS bands and NO_γ
12 bands, the OH ($A^2\Sigma^+(v') \rightarrow X^2\Pi(v'')$) system within 280–325 nm and the NH ($A^3\Pi(v') \rightarrow X^3\Sigma(v'')$)
13 transition centred at 336.0 nm can be found: Fig. 2 presents partially enlarged figures of OH (A→X)
14 transitions and NO_γ (A→X) bands.

1 **N₂/H₂O/CO₂ plasma.** In the N₂/H₂O/CO₂ plasma, the relative intensity of OH and NH bands is
2 reduced while a strong CN violet system ($B^2\Sigma \rightarrow X^2\Sigma$) is observed, indicating the breaking of C=O
3 chemical bonds and their recombination with nitrogen, presumably via N₂ excited states and N₂⁺.

4

5 **3.2 Effect of CO₂ addition**

6 Fig. 3 presents the effect of CO₂ concentration on the conversion of toluene and energy efficiency
7 of the plasma process with or without the presence of 16% H₂O (Reference to test I and II). Clearly,
8 increasing CO₂ concentration decreases the conversion of toluene in the plasma reforming regardless
9 of the steam addition, indicating that adding CO₂ somewhat suppresses the conversion of toluene.
10 Possibly, more electrons and excited nitrogen molecules produced in the plasma region could be de-
11 energized and consumed by CO₂ molecules, instead of toluene. As a result, part of the input energy
12 is used for the dissociation of CO₂ into CO. The promoting effect of excited N₂ molecules on CO₂
13 conversion was reported by Indarto et al. [52] using a knife-shaped gliding arc plasma system.
14 Moreover, Heijkers et al. [53] developed a chemical kinetics model to understand the plasma
15 chemistry in a CO₂/N₂ microwave plasma and reported that N₂ contributes to populating the lower
16 asymmetric levels of CO₂, leading to a higher CO₂ conversion when increasing N₂ fraction. In this
17 experiment, the formation of strong CN violet bands in the spectrum of the N₂/H₂O/CO₂ RGA plasma
18 demonstrates the interaction between CO₂ and excited N₂ in the plasma reforming of toluene (Fig. 2).
19 In addition, the decrease of excited nitrogen molecules also contributes to the decreased conversion
20 of toluene due to the reduced chance for the reaction of toluene with excited nitrogen species.

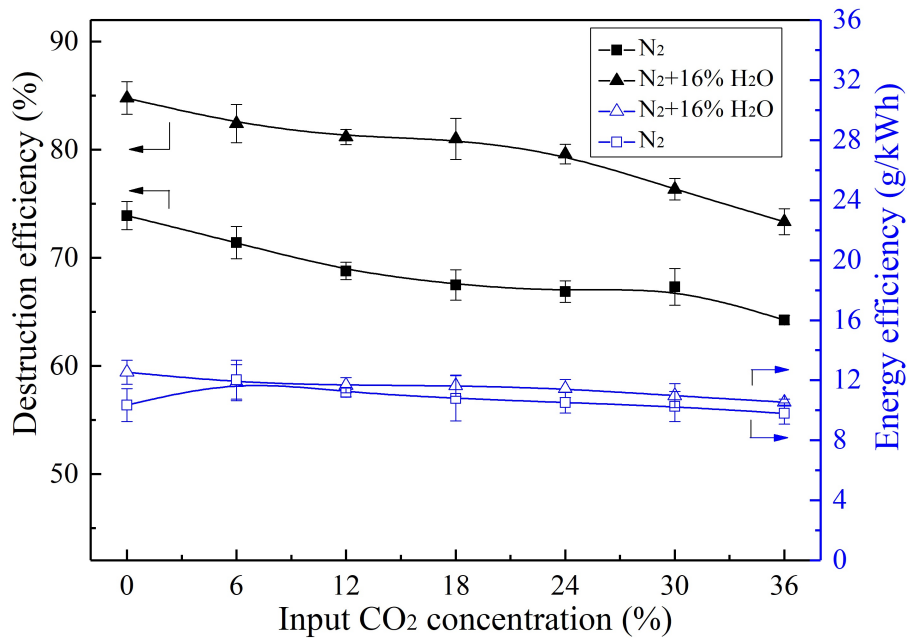


Fig. 3. Effect of input CO₂ concentration on the toluene conversion and energy efficiency (test I and II).

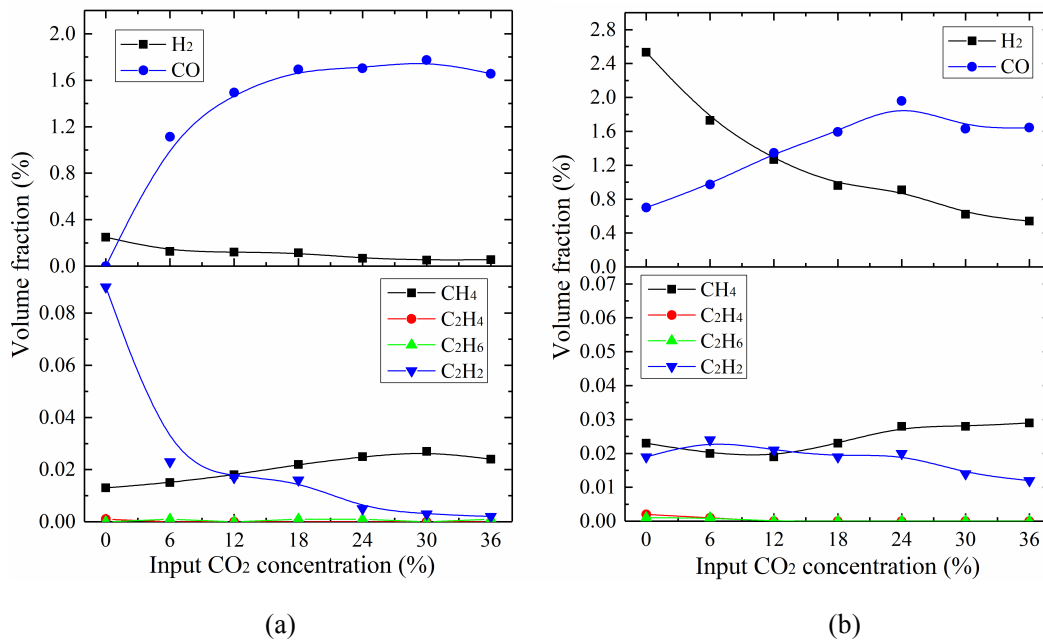


Fig. 4. Effect of input CO₂ concentration on gaseous products

(a) N₂ + CO₂ (test I), (b) N₂+16% H₂O + CO₂ (test II).

In addition, the energy efficiency of the process also decreases from 12.53 to 9.79 g/kWh when increasing CO₂ concentration with the presence of H₂O. Until now, limited efforts have been devoted to understanding the effect of gas composition on tar reforming. Pemen et al. [54] investigated the

1 individual effect of H₂O, CO₂ and H₂ on the removal of naphthalene using a pulsed corona discharge.
2 They found that the presence of CO₂ in the plasma reforming process costed more energy compared
3 to the addition of steam in the same process.

4 Fig. 4 shows the influence of CO₂ concentration on the volume fraction of gaseous products. H₂
5 and CO are found as major gas products. With the increase of CO₂ concentration, the volume fraction
6 of CO initially increases, reaching a peak at a CO₂ content of 24% and then slightly decreases,
7 regardless of the steam addition. By contrast, the volume fraction of H₂ is decreased when increasing
8 CO₂ concentration, which could be ascribed to the presence of reverse water-gas shift reaction (R1)
9 in the plasma tar reforming. An exception can be observed in Fig. 4(b) with the presence of 16% H₂O,
10 i.e., the CO volume fraction decreases with increasing CO₂ concentration to over 24%. This is
11 probably related to the significant drop in the conversion of toluene in these conditions (see Fig. 3)
12 that is caused by the excessive amounts of CO₂ added in the plasma system with the presence of 16%
13 H₂O (H₂O has a negative effect on toluene conversion at relatively high contents (see Section 3.3)).



15 In addition, a small amount of CH₄, C₂H₂, C₂H₄ and C₂H₆ are found in the gas phase. C₂H₂ and
16 CH₄ are the dominant hydrocarbons while the concentrations of C₂H₄ and C₂H₆ are almost negligible,
17 implying that the energy density of the RGA discharge is sufficiently high for stepwise
18 dehydrogenation of C₂H₆ and C₂H₄ to C₂H₂. Our previous modelling work has proved that the
19 electron impact dissociation of C₂H₆ and C₂H₄ can contribute significantly to the formation of C₂H₄
20 and C₂H₂, respectively [44]. A similar phenomenon was reported in plasma dry reforming of methane
21 and carbon dioxide in which C₂H₂ was found as the major hydrocarbon [20, 55]. The significant drop
22 of C₂H₂ fraction upon rising CO₂ concentration partially manifests that the reactive species produced
23 in the plasma region could be de-energized by CO₂ addition.

3.3 Effect of steam addition

Adding an appropriate amount of steam (Fig. 5) shows a positive influence on the conversion of toluene: gradually increases with rising steam concentration, reaching a maximum of 85.2% and 80.4% at a steam concentration of 16% in test III and IV, respectively, and then declines when further increasing steam content. Whereas, no significant influence of steam concentration on energy efficiency can be observed. In the presence of steam, numerous OH radicals are generated through the collision of H₂O with energetic electrons and excited N₂ species (see the OES spectra in Fig. 2). The generated OH radicals could oxidize toluene and reaction intermediates, creating new reaction pathways for direct and indirect destruction of toluene, and consequently enhanced the conversion of toluene and energy efficiency of the plasma reforming process, which can also be confirmed from both experimental and simulation studies [56-59].

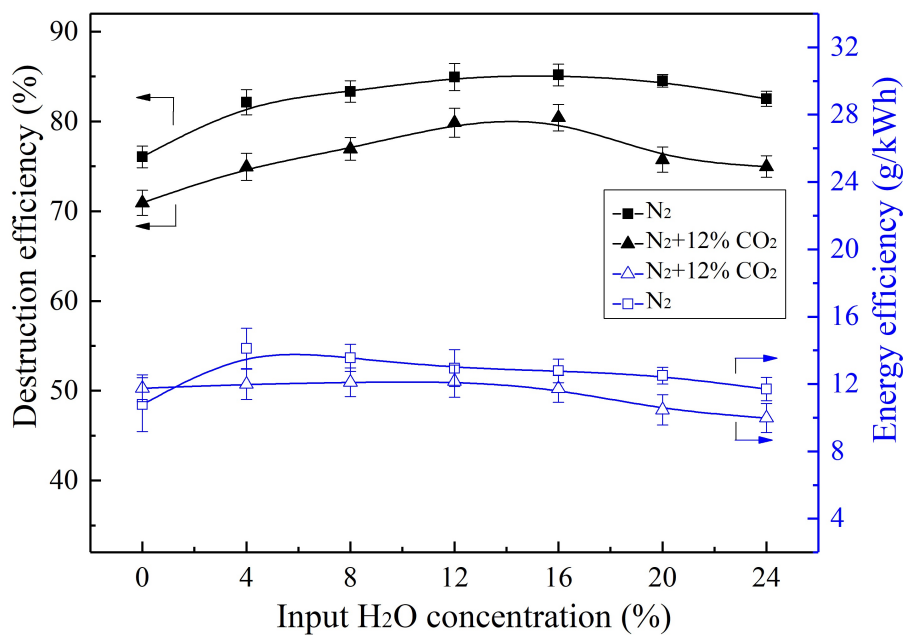
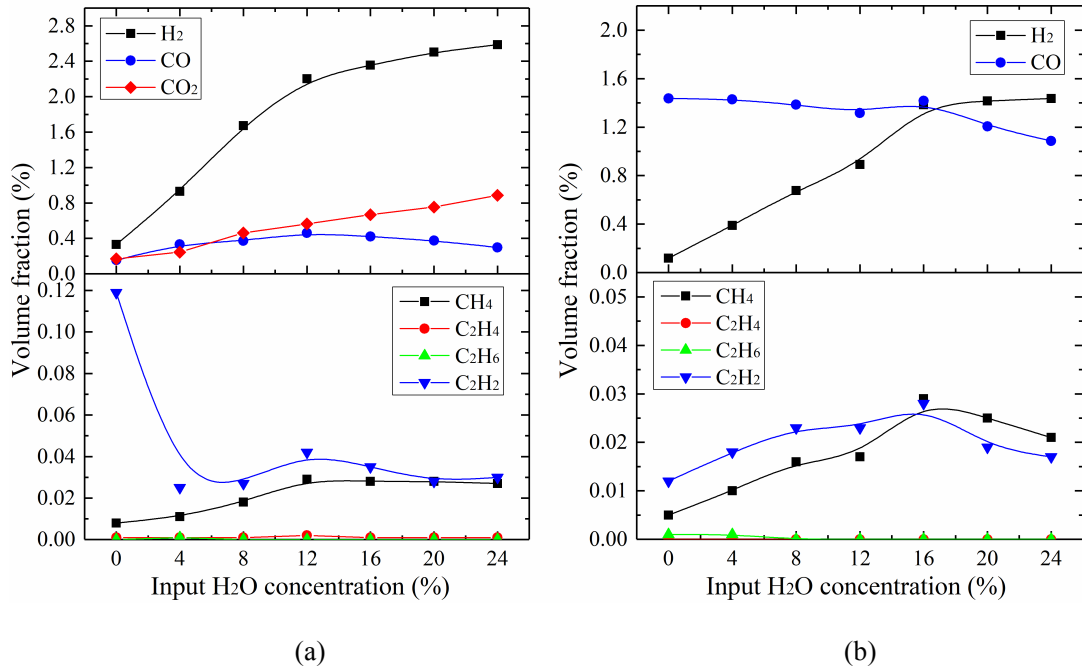


Fig. 5. Effect of input H₂O concentration on the toluene conversion and energy efficiency (test III and IV).

On the other hand, water also has an adverse effect on toluene conversion due to its electronegative characteristics. Too many H₂O molecules limit the electron density in the discharge region and quench

1 the reactive chemical species, causing a further decrease of the conversion and energy efficiency.
 2 Similar results were reported by Chun et al. [29] and Du et al. [60] when using gliding arc discharge
 3 for benzene and toluene decomposition, respectively. Note that the quenching effect of H₂O molecule
 4 on electrons and reactive species in the plasma system has been evidenced and extensively
 5 investigated [61-64].



6
7
8 Fig. 6. Effect of input H₂O concentration on gaseous product components

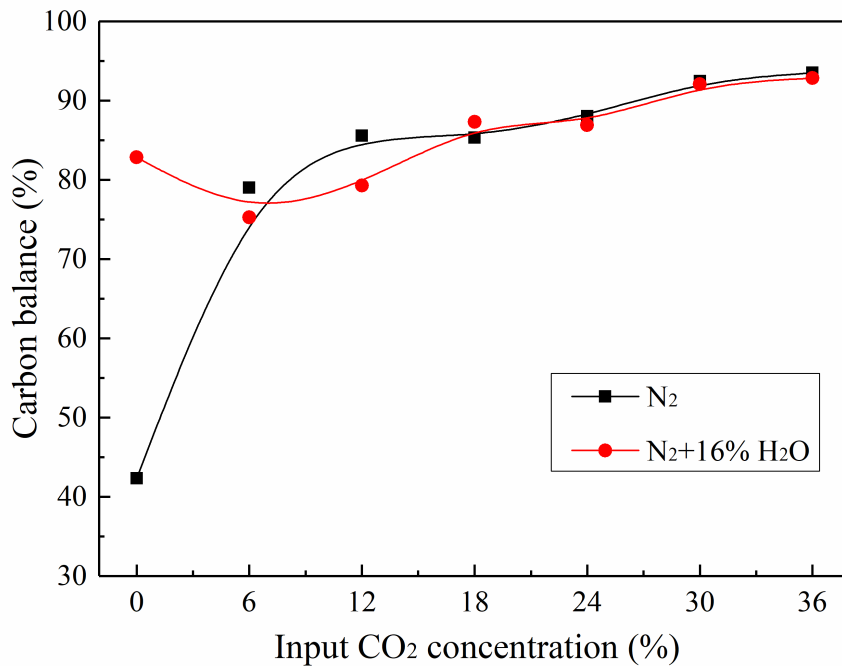
9 (a) N₂+H₂O (test III), (b) N₂+12%CO₂+H₂O (test IV).
10

11 Fig. 6 shows the effect of steam concentration on the production of gaseous products. In addition
 12 to H₂ and CO, CO₂ is found as one of the major products in the case of adding steam alone, as shown
 13 in Fig. 6a. With rising steam concentration, the water gas shift reaction (R2) plays a more important
 14 role in the reforming process, leading to the increased volume fraction of CO₂ and H₂, as well as the
 15 decreased CO formation. Note that an abrupt drop of the C₂H₂ volume fraction can be found in Fig.
 16 6a when the steam concentration changes from 0 to 4%. This is a favourable result since C₂H₂ has
 17 been proved to be a primary soot precursor during thermal cracking [65]. In the RGA plasma, C₂

1 intermediates can be sufficiently oxidized by OH radicals, and lead to subsequent reactions involving
2 CH₄ to form mainly CO, rather than soot. The concentration of CH₄ and C₂H₂ is less than 0.05%
3 under all test conditions with oxidants.



5 Fig. 7 presents the carbon balance as a function of the input CO₂ concentration. The balance merely
6 reaches 42.3% without the addition of steam or CO₂, due to the generation of a large amount of carbon
7 deposition. When adding CO₂ or H₂O, this problem is well solved and the carbon balance is almost
8 doubled as shown in Fig. 7, ensuring the stable operation of the RGA reactor. The addition of CO₂ or
9 H₂O increases the formation of oxidative species in the plasma that can suppress the formation of
10 carbon deposition.

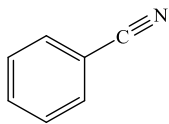
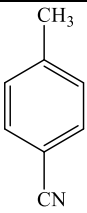
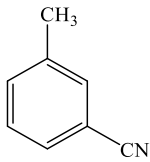
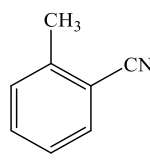
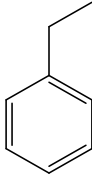
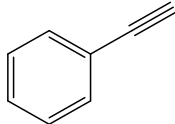
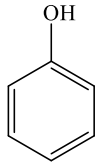
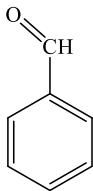
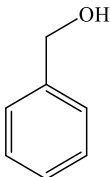
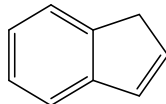
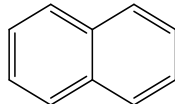


11
12 Fig. 7 Carbon balance versus input CO₂ concentration.

14 3.4 Reaction mechanisms

1

Table 1. Relevant liquid by-product structures identified by GC-MS.

Carrier gas	Specific by-products			General by-products		
N ₂						
	Benzonitrile	4-methyl -benzonitrile	3-methyl -benzonitrile	2-methyl -benzonitrile	Ethylbenzene	Phenylethyne
	N ₂ /CO ₂ /H ₂ O					
Phenol		Benzaldehyde	Benzylalcohol	Indene	Naphthalene	

2

3 To reveal the possible reaction pathways and mechanisms of toluene destruction in the RGA plasma,
4 the condensed liquid by-products with their relevant structures are listed in Table 1. Ethylbenzene,
5 phenylethyne, indene and naphthalene are the major monocyclic and bicyclic products formed in the
6 reaction regardless of the addition of steam or CO₂ ('general by-products' in Table 1). Trace amounts
7 of aliphatic compounds, such as decane and dodecane, are also detected in both cases. Their relevant
8 structures were already reported in our previous work [47]. Apart from these general by-products,
9 dissimilarities can be found among some N-compounds identified in the plasma reforming process
10 with and without using CO₂ and steam. When using pure N₂ as a carrier gas, benzonitrile and three
11 isomers of methyl-benzonitrile are formed through the recombination of CN radicals with phenyl or
12 with methylphenyl. However, in the N₂/CO₂/H₂O discharge, the presence of oxidative radicals in the
13 reaction produces oxygen-containing compounds such as phenol, benzaldehyde and benzylalcohol.
14 It should be noted that further detailed quantitative study of the liquid by-products is still needed to
15 confirm the above hypothesis.

16 The presence of reactive species is vital for cracking tar in a plasma. The main reaction mechanism

1 generally proceeds through three steps: (i) generation of reactive species; (ii) reactive species chain
2 reactions leading to tar destruction; and (iii) reactive species termination [54, 66]. According to the
3 steady-state hypothesis, postulating that similar numbers of radicals are created and removed, the
4 steps (i) and (iii) are often considered to be in balance. Equating their rates allows to formulate a
5 reaction rate expression and obtain the reaction order of the entire reaction system. Reactions (ii) are
6 much more frequent, and determine the chain length. They comprise H-abstraction reactions
7 involving reactive radicals and toluene, as well as reactions describing the further decomposition of
8 the resulting, still relatively stable radical. The latter can fragmentize by stepwise breaking of C-C-
9 bonds, rearrange, or even condense and polymerize, paving the way to further condensation,
10 dehydrogenation and carbonization, in brief ‘coking’.

11 Excited nitrogen molecules N_2^* , hydroxyl radicals OH and oxygen atoms O can be initially
12 produced following electron impact dissociation via reactions R3-R5. Besides, the generated N_2^* can
13 further facilitate the dissociation of water and carbon dioxide via reactions R6 and R7, as the energy
14 of the $N_2(A^3 \Sigma_u^+)$, $N_2(B^3 \Pi_g)$ and $N_2(a^1 \Sigma_u^-)$ states is high enough, with a value of 6.17 eV, 7.35 eV
15 and 8.4 eV, respectively.

16 Toluene conversion in an RGA plasma may proceed through H abstraction and consecutive
17 benzene ring cleavage; these reactions are induced by energetic electrons, excited nitrogen molecules
18 and free radicals via reactions R8-R16 [28, 57-59]. Trushkin et al. [58] developed a kinetic model of
19 toluene decomposition in a DBD plasma, suggesting that the direct contribution of the electron impact
20 decomposition of toluene does not exceed 2%, and the main channels of toluene decomposition in
21 pure N_2 are associated with metastable energetic $N_2(A^3 \Sigma_u^+)$ and $N_2(a^1 \Sigma_u^-)$ molecules.

22 In the presence of steam, the OH radicals make the largest contribution to toluene destruction [59].
23 Moreover, the OH radical creates an additional reaction route for toluene decomposition, starting with

1 the addition of OH to the aromatic ring through reaction R15 [28, 60]. In the presence of CO₂, the
 2 oxygen atoms generated by reactions R5 and R7 might also participate in decomposing toluene
 3 through reaction R16. However, compared to the reaction coefficient (6.16×10^{-12} cm³/mol•s, 298 K)
 4 of a hydroxyl radical OH with a toluene molecule (R14), the reaction between O atoms and toluene
 5 molecules is two orders of magnitude slower, with a reaction coefficient of 7.63×10^{-14} cm³/mol•s (298
 6 K) [67, 68].

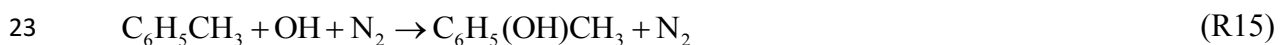
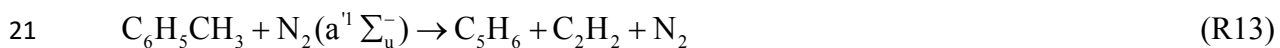
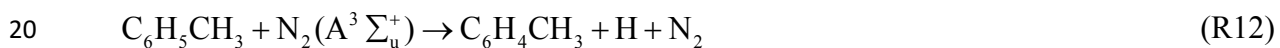
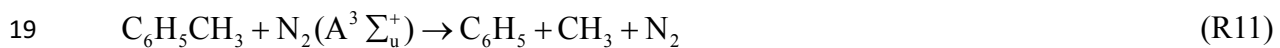
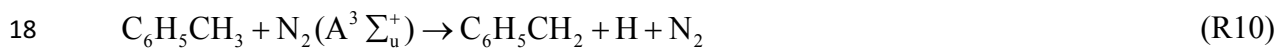
7

8 R3 to R7 represent the most obvious reactive species generating reactions



14

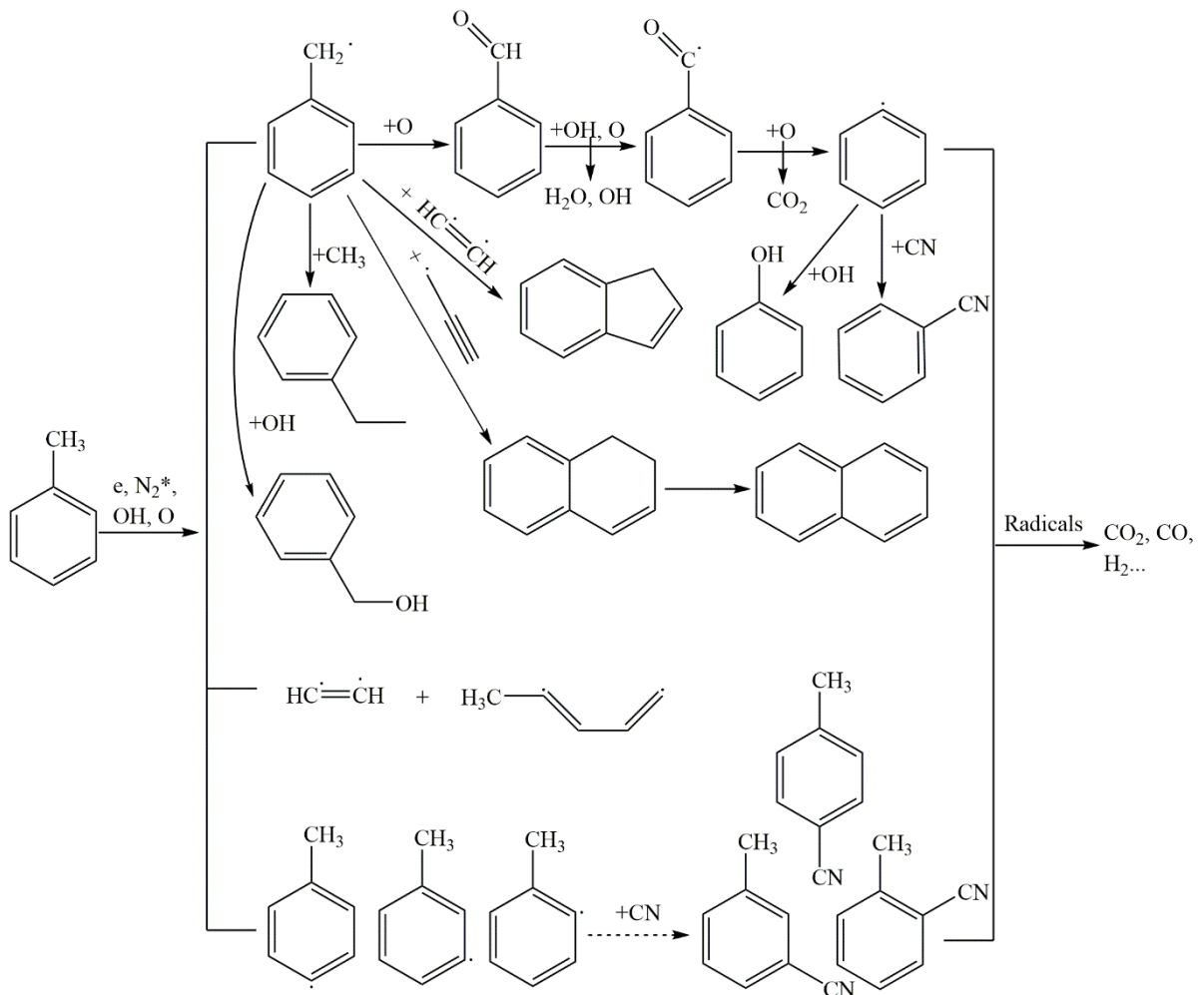
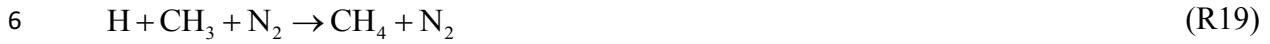
15 The tar destruction reactions centre on destabilizing toluene





2

3 Reactive species termination reactions



9

10

Fig. 8. Possible mechanisms of toluene destruction in the RGA plasma.

11

12 The possible reaction pathways for toluene destruction are schematically shown in Fig. 8, as based

1 on the aforementioned discussion. Initially, H atoms more easily derive by breaking a C-H bond from
2 the substituted methyl group via R8 and R10 than from the benzene ring, resulting in $C_6H_5CH_2$ or
3 benzyl radical generation. The radical rapidly interacts with O atoms, forming benzaldehyde
4 C_6H_5CHO , which is efficiently further oxidized by O atoms and OH radicals to form C_6H_5CO and
5 then the phenyl radical C_6H_5 .

6 Such a phenyl radical could easily react with OH and CN radicals, leading to the formation of
7 phenol and benzonitrile. Ethylbenzene and benzylalcohol, detected in the liquid samples by GC-MS,
8 can be produced from recombination of benzyl radicals with methyl radicals and OH radicals,
9 respectively.

10 The generation of indene suggests that toluene destruction is accompanied by reactions proceeding
11 with benzene ring cleavage and producing the bi-radical $HC=CH$ and methyl-cyclobutadiene via R13.
12 Indene can be composed by the recombination of benzyl radical and a bi-radical $HC=CH$, followed
13 by ring closure. Besides, bi-radicals $HC=CH$ could form acetylene through their rearrangement. The
14 main pathway for naphthalene formation is speculated to be the dehydrogenation of 1,2-
15 dihydronaphthalene, which could be formed by interactions of benzyl and propargyl radicals. The
16 three isomers of methyl-benzonitrile are generated from the recombination of CN radicals with
17 methylphenyl $C_6H_4CH_3$ produced through R12. An overwhelming majority of the aforementioned
18 intermediate products can be oxidized to final products (CO , H_2 and CO_2) through the interaction
19 with oxygen atoms and hydroxyl radicals. Moreover, the radical termination reactions (R17-R21) are
20 also responsible for the formation of gaseous products.

21 Moreover, thermal cracking of toluene probably exists in the RGA plasma system due to the
22 relatively high overall gas temperature of the plasma. Based on previous measurement results of using
23 a thermal couple and a thermal infrared imager, the gas temperature downstream the arc is lower than

1 800 °C Our experiments showed that the conversion of toluene by thermal decomposition only
2 reached 5.2% at a temperature of 800 °C (with a residence time of 0.17s in a tube furnace). Note that
3 in the RGA reactor, the total residence time of the injected gas in the chamber between the plasma
4 arc and the outlet was calculated to be around 0.24 s, which is comparable to that in thermal
5 decomposition experiments. However, it is still unclear how significantly the thermal effect plays a
6 role in the destruction of tar. There is currently no available technique to directly detect the gas
7 temperature inside the arc column, but as simulated by some authors, the gas temperature inside the
8 arc can be up to 2700 K [32]. That means thermal cracking of toluene may proceed inside and
9 surrounding the arc column. Further efforts of experiments and simulation are still needed to
10 understand the role of thermal effect in non-thermal assisted tar destruction process.

11

12 3.5 Comparison and further improvement

13 Table 2 shows a comparison of the performance of tar reforming using different non-thermal
14 plasmas. Clearly, each previous work using other non-thermal plasmas has at least one defect like
15 low conversion, low processing capacity (flow rate) or low energy efficiency, while the RGA shows
16 a relatively balanced performance. Compared to the DBD plasmas in [70-71], the RGA plasma could
17 offer a significantly higher processing capacity and a higher or comparable energy efficiency.
18 However, it is surprising that the DBD plasma in [27] exhibited almost the highest tar conversion
19 (96%) together with the highest energy efficiency (25%) even at a very high tar content (180 g/Nm³)
20 compared to other works (0.05-82 g/Nm³). Compared to microwave discharges, the RGA plasma has
21 higher energy efficiency and does not need a vacuum device. Also, note that the RGA reactor is more
22 feasible to be scaled up compared to the traditional flat GA, since its 3D geometry ensures a sufficient
23 mixing effect between the reactants and the plasma region.

1 From an economical viewpoint, the energy efficiency of plasma methods for tar elimination should
 2 be further improved. Nair et al. carried out a pilot test by coupling a pulsed corona reactor to a biomass
 3 gasifier and reported that 20% of the final electrical output from biomass gasification was used to
 4 power the plasma process [24]. Further improvement of tar conversion and energy efficiency can be
 5 expected by developing new reactor designs or using a pulsed power source which can significantly
 6 reduce the energy cost of the plasma process by a factor of four. In addition, the combination of the
 7 plasma with appropriate catalysts has great potential to generate a synergistic effect resulted from the
 8 interaction between the plasma and catalyst, which can significantly enhance the destruction of tars
 9 and syngas yield, as well as the energy efficiency of the process. Tao et al. combined a pulsed plasma
 10 with Ni catalysts for the destruction of toluene as a model tar and found that the conversion of toluene
 11 was almost doubled compared to the plasma reforming or catalytic reforming at the same temperature
 12 [40]. A synergistic effect between plasma and catalyst was also reported in our previous study by
 13 combining an RGA discharge with Ni catalysts for biogas reforming [55].

14
 15 Table 2. Comparison of tar elimination using different non-thermal plasmas

Plasma reactor	Tar compound	Tar content (g/Nm ³)	Working gas	Flow rate (Nm ³ /h)	Conversion (%)	Energy efficiency (g/kWh)	Reference
DC corona	Naphthalene	0.05	N ₂ /O ₂	0.3	35	3.2	[69]
DBD	Toluene	82	CO ₂	0.006	99	5.0	[70]
DBD	Benzene	36	CO ₂	0.0024	~99	14.0	[71]
DBD	Toluene	180	N ₂ /steam	0.009	96	25	[27]
Microwave	Pine tar	4.2	N ₂ /Ar	0.76	>99.0	4.5	[26]
GA	Toluene	23.5	N ₂ /steam	0.23	35.8	16	[28]
GA	Benzene	4.3	N ₂ /steam	1.00	82.6	20.9	[29]
GA	Naphthalene	1.3	N ₂	0.41	~70	~2.5	[72]
RGA	Toluene	10.0	N ₂ /steam	0.60	85.2	11.7	This work

1 It should be noted that, non-thermal plasma technology is recently emerging for tar reforming and
2 most of current studies in this field are focusing on the reforming of model tar compounds, such as
3 toluene and naphthalene, to test the performance of plasma used for tar reforming and to understand
4 the underlying mechanisms. However, to advance the practical application of this promising
5 technology, further studies on the application of plasma to a practical gasifier (or even bench scale
6 facility) for tar reforming under real gasification conditions are still urgently needed.

7 Compared with traditional physical or thermal methods for tar removal, the non-thermal plasma
8 technology shows unique merits of high specific productivity, high reaction rate, low investment cost,
9 and operation under mild conditions (i.e., atmospheric pressure and low temperature). This is
10 noteworthy, due to the property of instant on/off, the plasma processes can directly use the
11 intermittent renewable electricity, from wind and solar. It is commonly known that the curtailment of
12 generation is a normal occurrence in a renewable energy plant. Therefore, non-thermal plasma
13 technology is promising for tar reforming, especially when a renewable energy source can be used
14 for plasma generation, in which case the operation cost can be significantly reduced. The scale up of
15 plasma technology has been proved in some practical applications, such as polluted water treatment
16 [73]. The scale up can be realized mostly via the multiple reactors (or electrodes) in series but not via
17 the enlargement of a single reactor. However, before the plasma technology can be competitive to
18 traditional tar removal methods, further enhancement of the energy efficiency at a relatively high tar
19 conversion is still needed.

20

21 **4. Conclusion**

22 The influence of CO₂ and steam, two major oxidants in the producer gas, on the destruction of
23 toluene as a tar model compound in a novel RGA plasma reactor has been investigated in terms of

1 the conversion of toluene, gas production and the energy efficiency of the plasma process. The
2 presence of CO₂ in the plasma reforming reduces the destruction of toluene, while the addition of
3 appropriate steam enhances the conversion of toluene with a maximum toluene destruction of 85.2%
4 achieved at the optimal steam concentration of 16%. The presence of CO₂ or steam in the plasma
5 reforming process significantly reduces carbon deposition with syngas being the major gas products.
6 OES diagnostics shows the production of a range of reactive species which make a significant
7 contribution to the destruction of toluene and the reaction intermediates in the plasma reforming
8 process. The possible major reaction pathways of toluene destruction in the RGA plasma have been
9 proposed based on the analysis of gas and condensed liquid products combined with the emission
10 spectra of the RGA plasma under different conditions.

11

12 **Acknowledgement**

13 The support of this work by the National Natural Science Foundation of China (No. 51576174, No.
14 51706204 and No. 51621005), EPSRC SUPERGEN Bioenergy Challenge (Ref. EP/M013162/1),
15 EPSRC Impact Acceleration Account (IAA), Newton Advanced Fellowship (Ref. NAF/R1/180230)
16 and the Foundation of State Key Laboratory of Coal Combustion (No. FSKLCCA1805) is gratefully
17 acknowledged.

18

19 **References**

- 20 [1] Consonni S, Viganò F. Waste gasification vs. conventional Waste-To-Energy: A comparative evaluation of
21 two commercial technologies, *Waste Manage* 2012;32:653-666.
- 22 [2] Molino A, Chianese S, Musmarra D, Biomass gasification technology: The state of the art overview, *J Energy*
23 *Chem* 2016;25:10-25.
- 24 [3] Heidenreich S, Foscolo PU, New concepts in biomass gasification, *Prog Energ Combust* 2015;46:72-95.
- 25 [4] Lopez G, Artetxe M, Amutio M, Alvarez J, Bilbao J, Olazar M, Recent advances in the gasification of waste
26 plastics. A critical overview, *Renew Sust Energ Rev* 2018;82:576-596.
- 27 [5] Yung MM, Jablonski WS, Magrini-Bair KA. Review of catalytic conditioning of biomass-derived syngas,

- 1 Energy Fuels 2009;23:1874-1887.
- 2 [6] Li C, Suzuki K. Tar property, analysis, reforming mechanism and model for biomass gasification—An
3 overview, *Renew Sustain Energy Rev* 2009;13:594-604.
- 4 [7] Engvall K, Kusar H, Sjöström K, Pettersson LJ. Upgrading of raw gas from biomass and waste gasification:
5 Challenges and opportunities, *Top Catal* 2011;54:949-959.
- 6 [8] Devi L, Ptasiński KJ, Janssen FJJG. A review of the primary measures for tar elimination in biomass
7 gasification processes, *Biomass Bioenergy* 2003;24:125-140.
- 8 [9] Milne TA, Abatzoglou N, Evans RJ. Biomass gasifier "tars": Their nature, formation, and conversion, National
9 Renewable Energy Laboratory Golden, CO, (1998) <https://www.osti.gov/biblio/3726>.
- 10 [10] Han J, Kim H. The reduction and control technology of tar during biomass gasification/pyrolysis: An
11 overview, *Renew Sustain Energy Rev*. 2008;12:397-416.
- 12 [11] Anis S, Zainal ZA. Tar reduction in biomass producer gas via mechanical, catalytic and thermal methods: A
13 review, *Renew Sustain Energy Rev* 2011;15:2355-2377.
- 14 [12] Brandt P, Henriksen UB. Decomposition of tar in gas from updraft gasifier by thermal cracking, 1st World
15 Conference and Exhibition on Biomass for Energy and Industry, Sevilla, Spain, 5-9 June 2000.
- 16 [13] Nunnally T, Tsangaris A, Rabinovich A, Nirenberg G, Chernets I, Fridman A. Gliding arc plasma oxidative
17 steam reforming of a simulated syngas containing naphthalene and toluene, *Int J Hydrogen Energy* 2014;39:
18 11976-11989.
- 19 [14] Shen Y, Yoshikawa K. Recent progresses in catalytic tar elimination during biomass gasification or
20 pyrolysis—A review, *Renew. Sustain. Energy Rev* 2013;21:371-392.
- 21 [15] Qian K, Kumar A. Catalytic reforming of toluene and naphthalene (model tar) by char supported nickel
22 catalyst, *Fuel* 2017;187:128-136.
- 23 [16] Huang Q, Lu P, Hu B, Chi Y, Yan J. Cracking of model tar species from the gasification of municipal solid
24 waste using commercial and waste-derived catalysts, *Energy Fuels* 2016;30:5740-5748.
- 25 [17] Dou B, Gao J, Sha X, Baek SW. Catalytic cracking of tar component from high-temperature fuel gas, *Appl*
26 *Therm Eng* 2003;23:2229-2239.
- 27 [18] Shen Y, Zhao P, Shao Q, Takahashi F, Yoshikawa K. In situ catalytic conversion of tar using rice husk char/ash
28 supported nickel-iron catalysts for biomass pyrolytic gasification combined with the mixing-simulation in
29 fluidized-bed gasifier, *Appl Energy* 2015;160:808-819.
- 30 [19] Zhang Z, Liu L, Shen B, Wu C. Preparation, modification and development of Ni-based catalysts for catalytic
31 reforming of tar produced from biomass gasification, *Renew Sust Energ Rev* 2018;94:1086-1109.
- 32 [20] Tu X, Whitehead JC. Plasma dry reforming of methane in an atmospheric pressure AC gliding arc discharge:
33 Co-generation of syngas and carbon nanomaterials, *Int J Hydrogen Energy* 2014;39:9658-9669.
- 34 [21] Zhang H, Zhu F, Li X, Xu R, Li L, Yan J, Tu X. Steam reforming of toluene and naphthalene as tar surrogate
35 in a gliding arc discharge reactor, *J Hazard Mater* 2019;369:244-253.
- 36 [22] Zhang H, Li X, Zhu F, Cen K, Du C, Tu X. Plasma assisted dry reforming of methanol for clean syngas
37 production and high-efficiency CO₂ conversion, *Chem Eng J* 2017;310:114-119.
- 38 [23] Jiang N, Guo L, Qiu C, Zhang Y, Shang K, Lu N, Li J, Wu Y. Reactive species distribution characteristics and
39 toluene destruction in the three-electrode DBD reactor energized by different pulsed modes, *Chem Eng J*
40 2018;350:12-19.
- 41 [24] Nair SA, Pemen AJM, Yan K, van Gompel FM, van Leuken HEM, van Heesch EJM, Ptasiński KJ, Drinkenburg
42 AAH. Tar removal from biomass-derived fuel gas by pulsed corona discharges, *Fuel Process Technol*
43 2003;84:161-173.
- 44 [25] Nair SA, Yan K, Pemen AJM, van Heesch EJM, Ptasiński KJ, Drinkenburg AAH, Tar removal from biomass-
45 derived fuel gas by pulsed corona discharges. A chemical kinetic study, *Ind Eng Chem Res* 2004;43:1649-1658.
- 46 [26] Elliott RM, Nogueira MFM, Silva Sobrinho AS, Couto BAP, Maciel HS, Lacava PT. Tar reforming under a

- 1 microwave plasma torch, *Energy Fuels* 2013;27:1174-1181.
- 2 [27] Liu L, Wang Q, Ahmad S, Yang X, Ji M, Sun Y. Steam reforming of toluene as model biomass tar to H₂-rich
3 syngas in a DBD plasma-catalytic system, *J of Energy Inst* 2017;91:927-939.
- 4 [28] Liu S, Mei D, Wang L, Tu X. Steam reforming of toluene as biomass tar model compound in a gliding arc
5 discharge reactor, *Chem Eng J* 2017;307:793-802.
- 6 [29] Chun YN, Kim SC, Yoshikawa K. Decomposition of benzene as a surrogate tar in a gliding arc plasma, *Environ*
7 *Progress Sustain Energy* 2013;32:837-845.
- 8 [30] Kalra CS, Cho YI, Gutsol A, Fridman A, Rufael TS. Gliding arc in tornado using a reverse vortex flow, *Rev*
9 *Sci Instrum* 2005;76:025110.
- 10 [31] Indarto A, Yang DR, Azhari CH, Mohtar WHW, Choi J-W, Lee H, Song HK. Advanced VOCs decomposition
11 method by gliding arc plasma, *Chem Eng J* 2007;131:337-341.
- 12 [32] Wang W, Mei D, Tu X, Bogaerts A. Gliding arc plasma for CO₂ conversion: Better insights by a combined
13 experimental and modelling approach, *Chem Eng J* 2017;330:11-25.
- 14 [33] Fridman A, Nester S, Kennedy LA, Saveliev A, Mutaf-Yardimci O. Gliding arc gas discharge, *Prog Energ*
15 *Combust Sci* 1999;25:211-231.
- 16 [34] Zhang H, Li X, Zhu F, Bo Z, Cen K, Tu X. Non-oxidative decomposition of methanol into hydrogen in a
17 rotating gliding arc plasma reactor, *Int J Hydrogen Energ* 2015;40:15901-15912.
- 18 [35] Zhang H, Zhu F, Bo Z, Cen K, X. Li, Hydrogen production from methanol decomposition in a gliding arc
19 discharge plasma with high processing capacity, *Chem Lett* 2015;44:1315-1317.
- 20 [36] Snoeckx R, Bogaerts A. Plasma technology—a novel solution for CO₂ conversion?, *Chem Soc Rev*
21 2017;46:5805-5863.
- 22 [37] Zhang H, Zhu F, Li X, Cen K, Du C, Tu X. Enhanced hydrogen production by methanol decomposition using
23 a novel rotating gliding arc discharge plasma, *RSC Adv* 2016;6:12770-12781.
- 24 [38] Gangoli S, Gutsol A, Fridman A. A non-equilibrium plasma source: magnetically stabilized gliding arc
25 discharge: I. Design and diagnostics, *Plasma Sources Sci T* 2010;19:065003.
- 26 [39] Lee D, Kim K-T, Cha M, Song Y-H, Optimization scheme of a rotating gliding arc reactor for partial
27 oxidation of methane, *P Combust Inst* 2007;31:3343-3351.
- 28 [40] Tao K, Ohta N, Liu G, Yoneyama Y, Wang T, Tsubaki N, Plasma enhanced catalytic reforming of biomass tar
29 model compound to syngas, *Fuel* 2013;104:53-57.
- 30 [41] Marias F, Demarthon R, Bloas A, Robert-Arnouil J, Modeling of tar thermal cracking in a plasma reactor,
31 *Fuel Process Technol* 2016;149:139-152.
- 32 [42] Zhao B, Zhang X, Chen L, Qu R, Meng G, Yi X, Sun L, Steam reforming of toluene as model compound of
33 biomass pyrolysis tar for hydrogen, *Biomass Bioenerg* 2010;34:140-144.
- 34 [43] Świerczyński D, Libs S, Courson C, Kiennemann A, Steam reforming of tar from a biomass gasification
35 process over Ni/olivine catalyst using toluene as a model compound, *Appl Catal B-Environ* 2007;74:211-222.
- 36 [44] Zhang H, Wang W, Li X, Han L, Yan M, Zhong Y, Tu X. Plasma activation of methane for hydrogen
37 production in a N₂ rotating gliding arc warm plasma: A chemical kinetics study, *Chem Eng J* 2018;345:67-78.
- 38 [45] Zhang H, Zhu FS, Tu X, Bo Z, Cen KF, Li XD, Characteristics of atmospheric pressure rotating gliding arc
39 plasmas, *Plasma Sci Technol* 2016;18:473.
- 40 [46] Zhang H, Li XD, Zhang YQ, Chen T, Yan JH, Du CM, Rotating gliding arc codriven by magnetic field and
41 tangential flow, *IEEE T Plasma Sci* 2012;40:3493-3498.
- 42 [47] Zhu F, Li X, Zhang H, Wu A, Yan J, Ni M, Zhang H, Buekens A. Destruction of toluene by rotating gliding
43 arc discharge, *Fuel* 2016;176:78-85.
- 44 [48] Fridman A, Gutsol A, Gangoli S, Ju Y, Ombrello T, Characteristics of gliding arc and its application in
45 combustion enhancement, *J Propul Power* 2008;24:1216-1228.
- 46 [49] Gangoli S, Gutsol A, Fridman A. Rotating non-equilibrium gliding arc plasma disc for enhancement in ignition

- 1 and combustion of hydrocarbon fuels, Proc Int Plasma Chem Soc (ISPC) 2005;1042-1043.
- 2 [50] Benstaali B, Boubert P, Cheron B, Addou A, Brisset J, Density and rotational temperature measurements of
3 the OH and NO radicals produced by a gliding arc in humid air, Plasma Chem. Plasma P 2002;22:553-571.
- 4 [51] Jamróz P, Kordylewski W, Wnukowski M, Microwave plasma application in decomposition and steam
5 reforming of model tar compounds, Fuel Process Technol 2018;169:1-14.
- 6 [52] Indarto A, Choi J, Lee H, Song HK. Conversion of CO₂ by gliding arc plasma, Environ Eng Sci 2006;23:1033-
7 1043.
- 8 [53] Heijkers S, Snoeckx R, Kozák T, Silva T, Godfroid T, Britun N, Snyders R, Bogaerts A. CO₂ Conversion in a
9 microwave plasma reactor in the presence of N₂: Elucidating the role of vibrational levels, J Phys Chem C
10 2015;119:12815-12828.
- 11 [54] Pemen A, Nair SA, Yan K, Van Heesch E, Ptasinski KJ, Drinkenburg A. Pulsed corona discharges for tar
12 removal from biomass derived fuel gas, Plasmas Polymers 2003;8:209-224.
- 13 [55] Zhu F, Zhang H, Yan X, Yan J, Ni M, Li X, Tu X. Plasma-catalytic reforming of CO₂-rich biogas over Ni/ γ -
14 Al₂O₃ catalysts in a rotating gliding arc reactor, Fuel 2017;199:430-437.
- 15 [56] Gao J, Zhu J, Ehn A, Aldén M, Li Z. In-Situ non-intrusive diagnostics of toluene removal by a gliding arc
16 discharge using planar laser-induced fluorescence, Plasma Chem Plasma Process 2017;37:433-450.
- 17 [57] Blin-Simiand N, Jorand F, Magne L, Pasquiers S, Postel C, Vacher JR. Plasma reactivity and plasma-surface
18 interactions during treatment of toluene by a dielectric barrier discharge, Plasma Chem Plasma Process
19 2008;28:429-466.
- 20 [58] Trushkin AN, Kochetov IV. Simulation of toluene decomposition in a pulse-periodic discharge operating in a
21 mixture of molecular nitrogen and oxygen, Plasma Phys Rep 2012;38:407-431.
- 22 [59] Trushkin AN, Grushin ME, Kochetov IV, Trushkin NI, Akishev YS. Decomposition of toluene in a steady-
23 state atmospheric-pressure glow discharge, Plasma Phys Rep 2013;39:167-182.
- 24 [60] Du CM, Yan JH, Cheron B. Decomposition of toluene in a gliding arc discharge plasma reactor, Plasma Sources
25 Sci Technol 2007;16:791-797.
- 26 [61] Sarani A, Nikiforov AY, Leys C. Atmospheric pressure plasma jet in Ar and Ar/H₂O mixtures: Optical emission
27 spectroscopy and temperature measurements, Phys Plasmas 2010;17:063504.
- 28 [62] Bruggeman P, Iza F, Guns P, Lauwers D, Kong MG, Gonzalvo YA, Leys C, Schram DC., Electronic quenching
29 of OH (A) by water in atmospheric pressure plasmas and its influence on the gas temperature determination by
30 OH (A-X) emission, Plasma Sources Sci T 2009;19:015016.
- 31 [63] Hibert C, Gaurand I, Motret O, Pouvesle J. [OH(X)] measurements by resonant absorption spectroscopy in a
32 pulsed dielectric barrier discharge, J Appl Phys 1999;85:7070-7075.
- 33 [64] Zhang H, Zhu F, Li X, Cen K, Du C, Tu X. Rotating gliding arc assisted water splitting in atmospheric nitrogen,
34 Plasma Chem Plasma P 2016;36:813-834.
- 35 [65] Materazzi M, Lettieri P, Mazzei L, Taylor R, Chapman C. Tar evolution in a two stage fluid bed-plasma
36 gasification process for waste valorization, Fuel Process Technol 2014;128:146-157.
- 37 [66] Vreugdenhil BJ, Zwart R, Neeft JPA. Tar formation in pyrolysis and gasification, Energy Research Centre of
38 the Netherlands, 2009 <https://www.ecn.nl/docs/library/report/2008/e08087.pdf>.
- 39 [67] Atkinson R. Kinetics and mechanisms of the gas-phase reactions of the hydroxyl radical with organic
40 compounds under atmospheric conditions, Chem Rev 1986;86:69-201.
- 41 [68] Baulch DL, Cobos CJ, Cox RA, Frank P, Hayman G, Just T, Kerr JA, Murrells T, Pilling MJ, Troe J. Evaluated
42 kinetic data for combustion modeling. Supplement I, J. Phys Chem Ref Data 1994;23:847-848.
- 43 [69] Ni MJ, Shen X, Gao X, Wu ZL, Lu H, Li ZS, Luo ZY, Cen KF, Naphthalene decomposition in a DC corona
44 radical shower discharge, J Zhejiang Univ-SC A 2011;12:71-77.
- 45 [70] Saleem F, Zhang K, Harvey A, Role of CO₂ in the conversion of toluene as a tar surrogate in a nonthermal
46 plasma dielectric barrier discharge reactor, Energy Fuel 2018;32:5164-5170.

- 1 [71] Saleem F, Zhang K, Harvey A, Decomposition of benzene as a tar analogue in CO₂ and H₂ carrier gases,
2 using a non-thermal plasma, Chem Eng J 2019;360:714-720.
- 3 [72] Yu L, Li X, Tu X, Wang Y, Lu S, Yan J. Decomposition of naphthalene by dc gliding arc gas discharge, J.
4 Phys Chem A 2010;114:360-368.
- 5 [73] Sugai T, Nguyen PT, Maruyama T, Tokuchi A, Jiang W, The effect of scale-up of pulsed corona discharge for
6 treatment of pollution water sprayed in discharge gap, IEEE T Plasma Sci 2016;44:2204-2210.

7
8
9
10
11

Declarations of interest: none